CALCULATION OF THE PARAMETERS OF A KRYPTON AND HALOGEN-AGENT MIXTURE PLASMA FLOW

V.A. Serdyuk and V.P. Starodub

Institute of Electronic Physics,
the Ukraine National Academy of Sciences, Uzhgorod
Received July 26, 1995

Theoretical studies and optimization of the parameters of a krypton and F_2 *mixture plasma flow for its composition, density, and temperature have been done to maximize the output of the excimer* KrF_0* *molecules. We have found that the main contribution to the production of excimers near the throat of a nozzle comes from ion-ion recombination. An optimal stagnation temperature exists at which the output of the excimer molecules peaks regardless of the initial densities of gas flows. The following initial parameters of the* Kr + F_2 *plasma:* $N_{Kr} > 10^{18}$ cm^{-3}, T_0>1.5 10^4 K, *and* $N_{F_2} > 10^{16}$ cm^{-3} *yield* $N_{KrF^*} \geq 10^{14}$ cm^{-3}.

In recent years many theoretical and experimental papers[1–4] have appeared that consider a possibility of laser generation in a recombining plasma flow. The first data on the implementation of the idea of a plasma-dynamic laser (PDL) were published in Refs. 5–8. The excimer PDLs based on halides of inert gases are no less interesting and promising but scantily known. Until the present time we have found only the data of investigations of the excimer production efficiency in plasma flows.[9–12]

In this paper, a theoretical model of creating an active medium for an excimer KrF* plasma-dynamic laser is considered that involves the description of a krypton plasma flow along a supersonic nozzle, plasma cooling due to its expansion, and then mixing with F_2 at a certain distance from the throat of a nozzle. The model provides knowledge of the basic krypton plasma parameters upon entering a mixing region such as the concentration and temperature of the plasma species and the plasma flow velocity. In addition, it displays kinetics of processes in the mixing region producing the KrF* excimer molecules.

One-dimensional krypton plasma flow along a supersonic nozzle was considered. Plasma had many species and consisted of electrons, neutral atoms, and ions of different charge multiplicity in ground and excited states. All species have the Maxwell velocity distribution. Influence of viscosity, thermal conductivity, and diffusion was neglected. External electric and magnetic fields were absent.

Because of different types of the dependence of ionization and recombination rates on temperature, we may divide the entire flow into the following zones: a) equilibrium (in which the ionization rate is equal to the recombination one), b) kinetic (the ionization rate is much less than the recombination one), and c) frozen (both rates vanish). Zonal boundaries were determined by the relation between characteristic gas-dynamic τ_g, and recombination τ_r times. As gas-dynamic time, we took the transit time of the plasma having the velocity V across the throat H: $\tau_g = H/V$. Characteristic recombination time $\tau_r = 1/\beta N_e^2$, where N_e is the electron concentration and β is the recombination coefficient of the multiply charged ion. To calculate β, the expression derived in the diffusion approximation[3] was used.

Our calculations have shown that the region of transition from equilibrium flow to frozen one is very narrow for a wide range of variations of the plasma stagnation parameters. This allowed us to use a model of instantaneous freezing[13] in which the plasma flow is divided into two zones, namely, equilibrium and frozen ones. Transition occurs in “freezing points” and their location is determined from the equation

$$\tau_g = \tau_r. \quad (1)$$

Solution of this equation gives the temperature T_f at which the degree of ionization becomes frozen. For the given nozzle, working gas, and plasma stagnation parameters, T_f is constant. It determines the boundary between equilibrium and frozen zones of the plasma flow.

Results of numerical solution of Eq. (1) for the krypton plasma are shown in Fig. 1 as variations of the normalized freezing temperature ($Q_f = T_f/T_0$) vs. the stagnation parameters: temperature T_0 and concentration of heavy particles N_0. At low temperatures T_0, the flow may be considered frozen along the entire length of the nozzle, i. e., freezing occurs immediately after the start of plasma motion. At $T_0 \geq 8000$ K the freezing point shifts down along the nozzle and the equilibrium flow zone appears. Its length increases with increasing initial temperature and plasma concentration.

0235-6880/96/02 108-04 $02.00

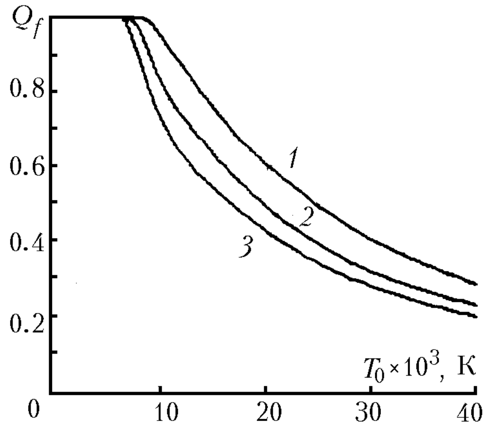

FIG. 1 Normalized freezing temperature of the Kr *plasma flow as a function of the stagnation parameters for a nozzle with height of throat* $H = 0.25$ cm *and* $N_{Kr} = 10^{18}$ *(1),* 10^{19} *(2), and* 10^{20} cm^{-3} *(3).*

Equations of plasma dynamics were solved for each zone of plasma independently and then joined in the freezing point. Gas dynamics and ion species of plasma in the equilibrium zone were described by the system of equations derived in Ref. 4 and completed by the Saha equation

$$\rho\, VA = \rho_*\, V_* = \text{const},\quad \rho\, V\text{d}V = -\,\text{d}P,$$

$$h + V^2/2 = h_0,\quad P = kT\,(N_g + N_e),$$

$$h = \frac{5}{2}\frac{kT}{m}\left[1 + \frac{N_e}{N_g}\right] + \frac{1}{m}\sum_{z=1}^{M}\frac{N_z}{N_g} I_z, \qquad (2)$$

$$\rho = m\,N_g + m_e\,N_e,$$

$$N_g = \sum_{z=0}^{M} N_z,\quad N_e = \sum_{z=1}^{M} N_z,$$

$$N_z = \frac{N_{z-1}}{N_e}\frac{2q_z}{q_{z-1}}\left[\frac{m_e\,kT}{2\pi\,h}\right]^{3/2}\exp\left[-\frac{I_z}{kT}\right],$$

where $A = S/S^*$ is the relative nozzle cross section, P is the pressure, m_e and m are the electron and krypton atom masses, respectively, q is the statistical weight of the ground state of the Z-multiply charged ions, h is the enthalpy, I_z is the ionization potential, N_z is the concentration of the Z-multiply charged ions, ρ^* and V^* are the density and velocity of the flow in the throat of the nozzle.

In the frozen zone of flow, the plasma composition remained unchanged and the plasma parameters in the nozzle were determined by the well-known gas-dynamic functions for isentropic flow[4]

$$\rho\, VA = \rho_*\, V_* = \text{const},\quad \rho = \rho_f\,[T/T_f]^{3/2},$$

$$h + V^2/2 = h_0,\quad P = kT\,N_g + kT_e\,N_e,$$

$$h = \frac{5}{2}\frac{k}{m}\left[T + T_e\frac{N_e}{N_g}\right] + \frac{1}{m}\sum_{z=1}^{M}\frac{N_z}{N_g} I_z,$$

$$N_g = N_{gf}\,\rho/\rho_f,\quad N_e = N_{ef}\,\rho/\rho_f,\quad N_z = N_{z\,f}\,\rho/\rho_f,$$

$$T_e = T + \Delta T(T_e, N_e), \qquad (3)$$

where ΔT_e is determined from a balance between the electron energy losses due to elastic collisions and recombination heating and is connected with the plasma parameters by the equation[4]

$$\Delta T_e = 0.57\cdot 10^{-6}\,(\mu\,\bar{Z}/\Lambda)\,(E^*\,N_e/T_e^3). \qquad (4)$$

Here, E^* is the effective recombination energy,[4] μ is the molecular weight, Λ is the Coulomb logarithm,

$$\bar{Z} = \frac{1}{N_e}\sum_{z=1}^{M} Z^2\,N_z \qquad (5)$$

is the average multiplicity of ionization. The subscript f refers to the parameters in the freezing point.

For this model we calculated the parameters of the Kr plasma flow in a planar supersonic wedge-shaped nozzle for different equilibrium conditions in a prenozzle camera and different nozzle geometry. The electron concentration and temperature distributions as well as the density and temperature of heavy species along the nozzle at constant initial density and different initial temperatures are shown in Figs. 2 and 3.

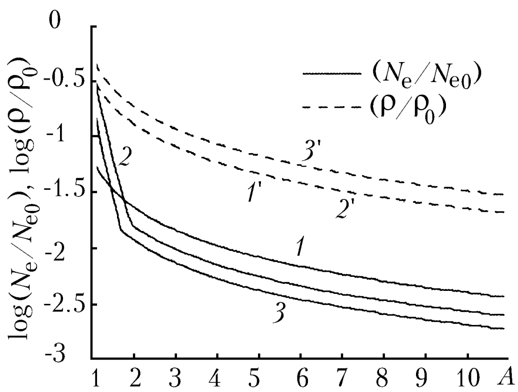

FIG. 2. Distribution of the Kr *plasma density and the electron concentration along a nozzle with height of throat* $H = 0.25$ cm *at* $N_{Kr} = 10^{18}$ cm^{-3} *and* $T_0 = 5000$ *(1 and 1′),* 10000 *(2 and 2′), and* 21000 K *(3 and 3′).*

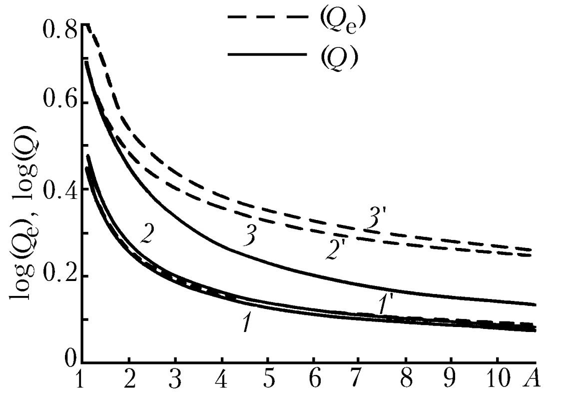

FIG. 3. Distribution of the electron temperature and heavy species of the Kr *plasma along a nozzle with height* $H = 0.25$ cm *at* $N_{Kr} = 10^{18}$ cm^{-3} *and* $T_0 = 5000$ *(1 and 1′),* 10000 *(2 and 2′), and* 21000 K *(3 and 3′).*

First of all, we call attention to the weak dependence of the plasma density along the nozzle on the initial conditions. The density profile for all calculated variants remained practically unchanged (see Fig. 2). The freezing efficiency of nozzle decreases with the increase of initial temperature T_0 and N_e/N_{e0} decreases sharply. At low initial temperatures (T_0 < 5000 K), Q_f is close to unity and the ratio N_e/N_{e0} is closely correlated with the profile of the plasma density (ρ/ρ_0) along the nozzle. Influence of recombination on the temperature is insignificant because of small ionization degree ($\alpha \cong 10^{-5}$) and we observe coincidence of Q and Q_e at the input of the nozzle (see Fig. 3, curves *1* and *1*′). A small discrepancy in temperatures Q and Q_e with the further expansion in the nozzle is due to the increasing recombination rate upon cooling and decreasing elastic energy exchange.

The increase of the stagnation temperature up to 10000 K leads to higher degree of plasma nonisothermicity due to recombination heating (see Fig. 3, curves *2* and *2*′) although the temperature profiles of heavy species in variants *1*, *1*′, *2* and *2*′ are close.

The further increase of the initial temperature (see Fig. 3, curves *3* and *3*′) leads to the decrease of the temperature nonequilibrium and deterioration of the cooling efficiency of the nozzle (cf. curves *2*, *2*′, *3*, and *3*′).

Processes in the mixing zone were described by the system of the velocity equations

$$dN_m/dt = \sum_{m'\neq m} N_m\, k_{mm'}\, N_{m'} , \qquad (6)$$

where N_m and $N_{m'}$ are the concentrations of interacting species of the mixture of Kr, Kr*, Kr^+, KrF*("), KrF_0^* ("), KrF (X), F_2, F^-, e, $h\omega$. In calculations we considered the upper vibrational levels of the KrF_0*(") molecule (ν=4–∞) to be populated by ion-ion recombination and harpoon reaction as well as by energy transfer from different species of the medium. A group of lower vibrational levels (ν=0–3) of the KrF_0*(") molecule, from which lasing occurs, is populated as a result of vibrational relaxation allowing for quenching collisions. The radiative decomposition of the KrF*(") and KrF_0*(") molecules occurs as a result of spontaneous and induced transitions to the KrF(X) state with subsequent decomposition of the molecule into atoms. We also considered the absorption of emitted photons by the KrF(X) molecule and other species of mixture.

The results of calculation of the KrF_0*(") population vs. the stagnation temperature of the Kr plasma flow and halogen (F_2) concentration in the zone of mixing of two flows are shown in Fig. 4. The numbers adjacent to curves indicate log (KrF_0*, cm^{-3}). In calculations the Kr concentration in the prenozzle camera was $N_{Kr} = 10^{19}$ cm^{-3}. Mixing was carried out at a distance of 3 mm from the throat of the planar wedge-shaped nozzle with a half-angle of 7^0 at its apex.

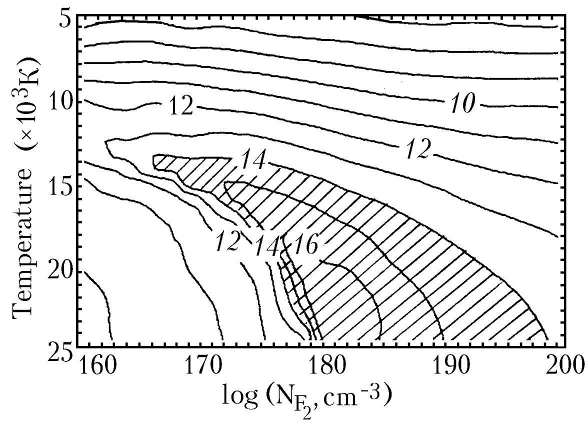

FIG. 4. Dependence of the output of the Kr *excimer molecules on the* Kr *stagnation temperature and the* F_2 *concentration in the mixing region.*

As is seen from Fig. 4, the output of the excimer molecules first increases with the increase of the stagnation temperature, reaches its maximum, and then decreases. The increase of the excimer concentration with the temperature increase is primarily due to the increase of Kr ion and electron concentration. The maximum output is followed by the decrease of the efficiency of production of the KrF_0* molecules caused by quenching processes, primarily, by the electrons.

The optimal ratio of the Kr^+(Ne) ion to halogen (F_2) concentration is close to unity. As temperatures increase up to the values at which the maximum concentration of the KrF_0*(") molecules occurs, the electron contribution to quenching of the excimer molecules becomes insignificant because the electron concentration becomes small due to intensive attachment of electrons to the F_2 molecules and production of the stable negative ion F^-. The further increase in the temperature at constant F_2 concentration leads to a surplus of the electron concentration resulting in the decrease of the KrF_0*(") concentration. Dominating contribution to the production of the excimer molecules comes from ion-ion recombination.

In Fig. 4 the range of variations of the initial parameters promising for obtaining laser generation in the plasma flow is hatched.

REFERENCES

1. I.R. Hurle and A. Hertzberg, Phys. Fluids **8**, No. 9, 1601–1607 (1965).
2. L.I. Gudzenko, S.S. Felipov, and L.A. Shelepin, Zh. Eksp. Teor. Fiz. **51**, No. 4, 1115–1119 (1966).
3. L.I. Gudzenko and S.I. Yakovenko, *Plasma Lasers* (Atomizdat, Moscow, 1978), 253 pp.
4. G.A. Luk'yanov, *Supersonic Plasma Flows* (Mashinostroenie, Moscow, 1985), 264 pp.
5. E.M. Campbell, R.G. Jahn, W.F. Jaskowsy, et al., J. Appl. Phys. **51**, No. 1, 109–117 (1980).
6. T. Hara, K. Kodera, M. Hamagaki, et al., Jap. J. Appl. Phys. **19**, No.10, 606–608 (1980).
7. I.I. Murav'ev, A.M. Shevnin, A.M. Yancharina, et al., Kvant. Elektron. **9**, No. 4, 793–796 (1982).
8. V.S. Rogulich, V.P. Starodub, and V.S. Shevera, Pis'ma Zh. Tekhn. Fiz. **12**, No. 10, 606–609 (1986).
9. V.S. Rogulich, V.P. Starodub, and V.S. Shevera, Zh. Tekhn. Fiz. **58**, No. 10, 1893–1896 (1988).
10. V.S. Rogulich, V.P. Starodub, and V.S. Shevera, Opt. Spektrosk. **69**, No. 4, 756–758 (1990).
11. V.T. Mikhel'soo, A.B. Treshchalov, V.E. Peet, et al., Kvant. Elektron. **14**, No. 7, 1404–1406 (1987).
12. V.A. Barinov, Yu.V. Geras'ko, O.F. Kostenko, et al., Zh. Tekhn. Fiz. **63**, No. 2, 65–73 (1993).
13. S.V. Makarychev, "*Experimental and theoretical study of the conditions of formation of an active medium in a supersonic flow of highly ionized plasma,*" Author's Abstract of Cand. Phys.-Math. Sci. Dissert., Moscow State University (1989), 16 pp.
14. A.G. Molchanov, Tr. Fiz. Inst. Akad. Nauk SSSR, **171**, 54–127 (1986).